




Novel Three-port Buck-Boost DC-DC Converter for Hybrid Vehicle Powertrains Capable of Returning Regenerative braking Energy

H. Soltani Gohari^{1*}, K. Abbaszadeh² 

¹ Department of Electrical Engineering, K.N.Toosi University of Technology, Tehran, Iran

² Professor, Department of Electrical Engineering, K.N.Toosi University of Technology, Tehran, Iran

ARTICLE INFO	ABSTRACT
<p>Article History: Received 9 March 2019 Received in revised form 2 April 2019 Accepted 15 June 2019 Available online 16 June 2019</p>	<p>The paper introduces a novel three-port buck-boost DC-DC converter designed for application in hybrid electric vehicle (HEV) powertrains. Notably, the converter's unique feature lies in its ability to function as a buck-boost converter in two directions, facilitating the recovery of regenerative braking energy during diverse driving cycles characterized by varying braking durations. The operating modes of the converter encompass charging, propulsion, and regenerative braking. While the battery can be charged using any DC power source such as a photovoltaic (PV) panel or rectified grid voltage, the paper specifically assumes a PV panel as the power source. This emphasis underscores the converter's versatility in accommodating a broad range of voltages. In propulsion mode, the converter can operate with one or two power sources in accordance with commands from the energy management system. To validate the system analysis, the proposed converter undergoes simulation in MATLAB software, covering different conditions within each operating mode. The simulation results are meticulously analyzed, providing a comprehensive understanding of the converter's performance under varied scenarios. This research contributes to advancing the capabilities of HEV powertrains, offering a versatile and efficient solution for energy management and regenerative braking in diverse driving conditions.</p>
<p>Keywords: DC-DC Converter, Hybrid Electric Vehicle, Hybrid Powertrain, Regenerative braking, Battery Charger</p>	

1. INTRODUCTION

Growing concerns regarding environmental issues such as global warming and the depletion of fossil fuels have spurred increased interest in Electric Vehicles (EVs). Car designers have explored various types of EVs [1-3], including Hybrid EVs (HEVs), Plug-in HEVs (PHEVs), Battery-powered EVs (BEVs), and Fuel cell HEVs (FCHEVs). While BEVs offer advantages such as a simple control system and zero-emission operation, limitations such as a restricted driving range and lower reliability have constrained their widespread adoption. This has led to the prevalence of Plug-in HEVs (PHEVs) over BEVs [4-6].

In FCHEVs, the powertrain utilizes multiple power sources to meet the required power demands. Depending on the designer's perspective, there is typically a primary power source and one or more auxiliary power sources. The

* Corresponding Author: Hsoltani@email.kntu.ac.ir

Department of Electrical Engineering, K.N.Toosi University of Technology, Tehran, Iran



efficient design of powertrain components is crucial for achieving high efficiency and optimal vehicle performance. Among these components, the DC-DC converter, interfacing between the power sources and the motor drive system, holds significant importance [7]. Properly regulating the voltage of the power sources, operating as a buck-boost converter, enabling bidirectional power flow, and efficiently recovering regenerative braking energy are crucial features that must be considered during the design of the DC-DC converter. These considerations play a vital role in determining the overall operation and efficiency of the entire system.

While various studies have explored converter topologies, only a few meet the comprehensive capabilities mentioned above. In [8], a coupled inductor-based soft-switching bidirectional DC-DC converter is proposed, particularly applicable in Hybrid Electric Vehicles (HEVs). Despite its advantages, such as soft-switching operation, it remains a single-input converter, necessitating multiple units in multi-source Electric Vehicles (EVs). Bidirectional DC-DC converters introduced in [9-11] lack the ability to both decrease and increase voltage levels in both directions, limiting their efficiency in HEVs.

Moreover, on-board chargers proposed in [12-13] are restricted to charging mode and lack the capacity to operate in propulsion and regenerative modes. Addressing these limitations, this paper introduces a multi-input bidirectional buck-boost DC-DC converter designed for use in Fuel Cell Hybrid Electric Vehicles (FCHEVs). The proposed converter operates seamlessly in charging, propulsion, and regenerative braking modes, eliminating the need for an additional converter in the powertrain.

A noteworthy feature of the introduced converter is its ability to function as a buck-boost converter in both directions, making it adaptable to various driving cycles with different braking conditions. This paper specifically employs a Photovoltaic (PV) panel for the charging mode, but it can easily be substituted with any DC power source, especially rectified grid voltage, showcasing its flexibility and compatibility with different energy sources.

2. TOPOLOGY AND OPERATION

The structure of proposed converter is shown in Fig.1. This converter works in three types of operating:

Battery charging (Mode1): in this operating mode, the converter charges the plugged vehicle’s battery with employed roof-top PV panel. Propulsion (Mode2 and Mode3): the proposed converter can feed the motor drive system with battery or battery and FC, simultaneously, depending on the energy management center commands. Due to the converter ability to work in buck-boost condition, in a wide voltage range of battery pack, the converter can handle the motor load properly. In this EV powertrain it is assumed that the battery is the main source.

Regenerative braking (Mode4): the proposed converter has the capability of returning the regenerative braking energy to the battery. Owing to its buck-boost structure it can do the regeneration task in different driving cycles. It is also designed in a way to have the ability to switch between propulsion and braking conditions rapidly.

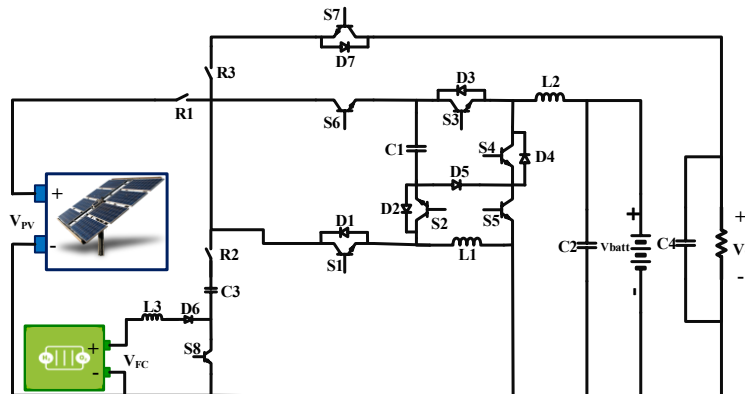


Fig. 1. Topology of proposed converter

The operation principle of each mode are explained and analyzed in following sections in detail.

Mode1 (Battery charging): In order to charge the battery with connector PV panel, the R1 relay is ON and R2 and R3 are OFF. In this condition, the converter is controlled depending on the PV voltage and battery cells SOC. The operation of this mode is divided into two states:

State1 ($0 < t < DT_s$): in this state S1, S2, and S3 are ON so L1 and L2 are magnetized with (V_{PV}) and $(V_{PV} + V_{C1} - V_{batt})$, respectively, and the switching capacitor, C1, is discharged [Fig.2 (a)].

State2 ($DT_s < t < T_s$): at $t = DT_s$ S1, S2, and S3 are turned OFF and S6 is turned ON so D2 is directly biased and C1 is charged with $(V_{PV} - V_{L1})$, consequently. L1 and L2 are demagnetized with $(V_{PV} - V_{C1})$ and $(V_{PV} - V_{C1} - V_{batt})$, respectively [Fig.2 (b)].

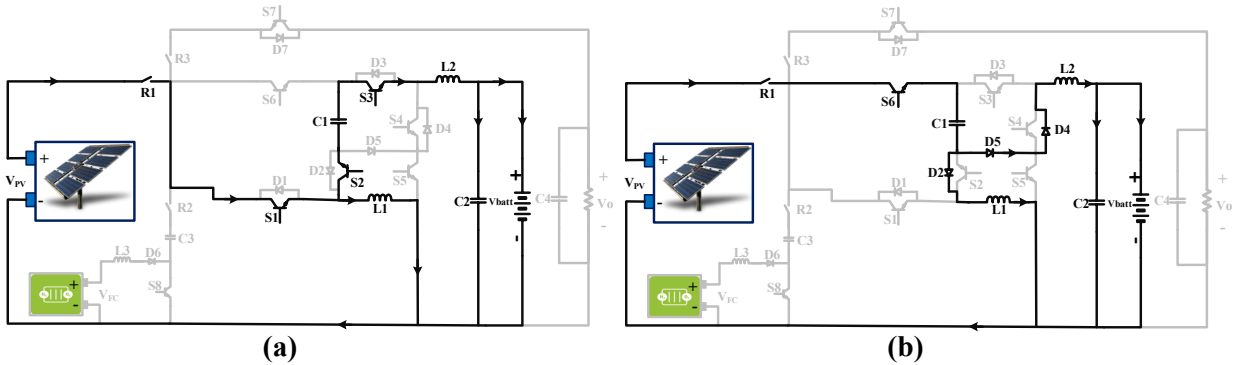


Fig. 2. Current paths and switch states in mode1

Mode2 (Propulsion with battery): In this mode, the converter provides the motor demanded power with battery. An impressive feature of the proposed converter is the ability working as a buck-boost converter which enables it to bypass the low-SOC battery cells by using CEC. The operation states are explained below:

State1 ($0 < t < DT_s$): in the first state, S2, S3, S4, and S5 are ON so L1 is magnetized with C1 energy. L2 is magnetized with V_{batt} . In this condition D1 and D7 are reversely biased [Fig.3 (a)].

State2 ($DT_s < t < T_s$): this state is the time for demagnetizing of L1 and L2. By turning OFF all switches except S5, the diodes D1, D3, D5, and D7 are directly biased consequently so L1 and L2 are demagnetized with $(-V_o)$ and $(V_{batt} - V_{C1})$, respectively [Fig.3 (b)].

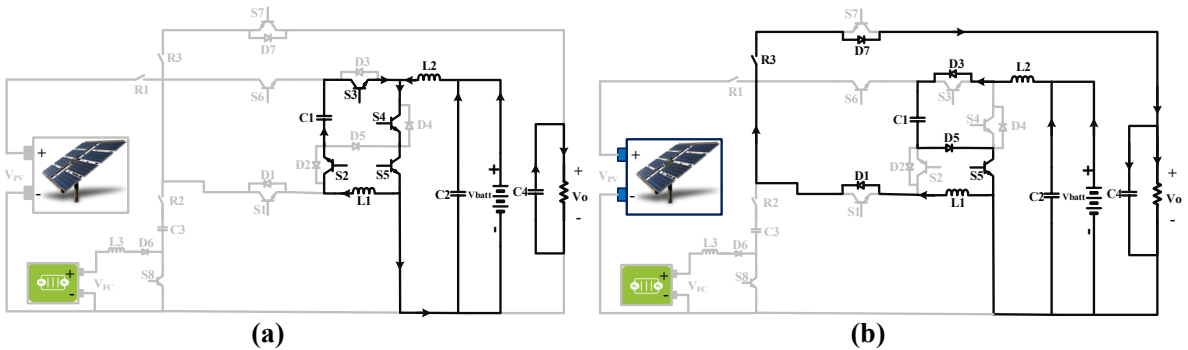


Fig. 3. Current paths and switch states in mode2

Mode3 (propulsion with battery and FC): if the FC stack has the ability to deliver power, the converter handles the load with battery and FC, simultaneously. According to the EMS center commands and SOC of battery cells, the voltage of battery can be regulated.

State1 ($0 < t < DT_s$): at the beginning of this state, S2, S3, S4, S5, and R2 are ON. L1 is magnetized with (VC1) and L2 is magnetized with V_{batt} . In this condition D6 and D7 are directly biased so C4 is charged with energy of FC, L3, and C3 [Fig.4 (a)].

State2 ($DT_s < t < Ts$): by turning OFF the S2, S3, and S4 and also turning ON the S8, D1 is directly biased and D7 is reversely biased. L1 is demagnetized with (-VC3) and L2 is demagnetized with ($V_{batt}-VC1$). The L3 is magnetized with (VFC) [Fig.4 (b)].

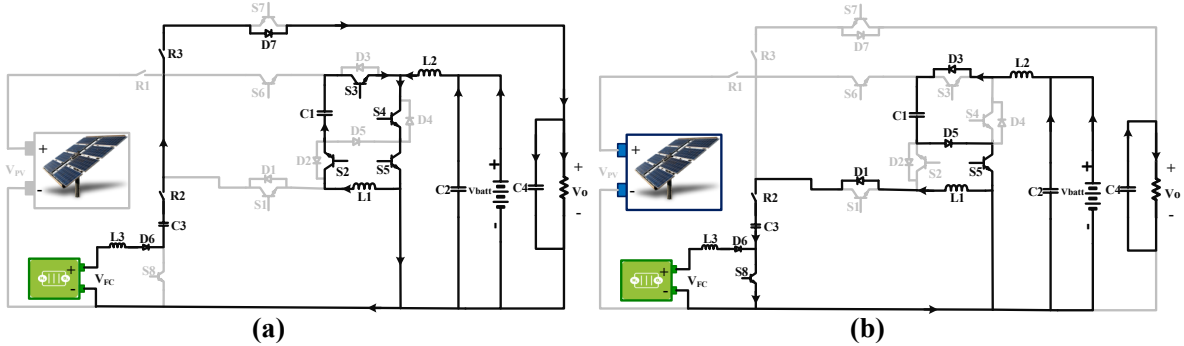


Fig. 4. Current paths and switch states in mode3

Mode4 (Regenerative braking): during vehicle braking, it is possible to return the regenerative energy and store that in battery. The amplitude of the motor drive system voltage can be different during braking times. The proposed converter can regulate this voltage over different driving cycles due to its buck-boost topology.

State1 ($0 < t < DT_s$): in this state, S1, S2, S3, and S7 are ON L1 and L2 are magnetized with (V_o) and ($V_o+VC1-V_{batt}$), respectively [Fig.5 (a)]. The switching capacitor, C1, is discharged in this state.

State2 ($DT_s < t < Ts$): at $t=DT_s$, the opened switches turned OFF and S6 is turned ON so L1 and L2 demagnetized with (V_o-VC1) and ($V_o-VC1-V_{batt}$), respectively. The C1 is charged in this mode [Fig.5 (b)].

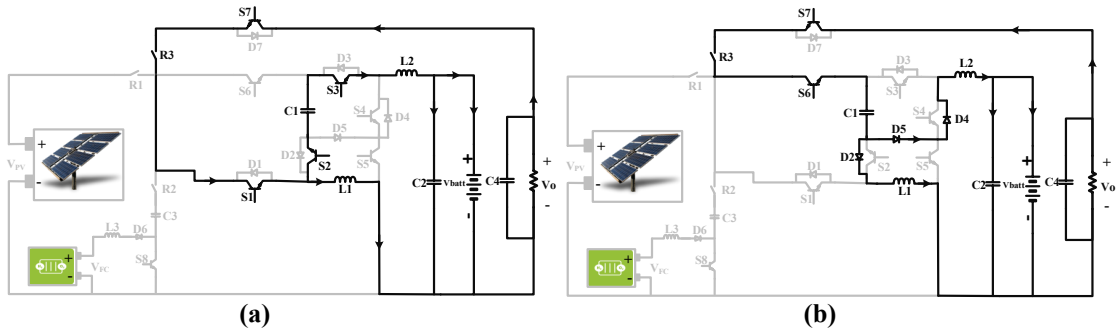


Fig. 5. Current paths and switch states in mode4

3. INVESTIGATE STEADY-STATE PERFORMANCE

In this section the steady-state performance of proposed converter is analyzed and voltage and current across inductive and capacitive components are obtained in addition to the voltage gain in each operating mode. In order to simplify the description of Time-domain analysis of the proposed converter, the following assumptions are considered:

- All passive components are ideal
- All switching devices are ideal (without voltage drop during ON-state)
- Resistive and energy storage components are linear time invariant

- Capacitance of C1, C2, C3, and C4 is large enough to keep voltage steady.

Mode1:

The status of switches and current of L1 are show in Fig.2 .From KVL identities, the voltages across inductive components L1 and L2 are obtained as:

for $0 < t < DT_s$:

$$\begin{cases} V_{L1} = V_{PV} \\ V_{L2} = V_{PV} + V_{C1} - V_{battery} \end{cases} \quad (1)$$

d for $DT_s < t < T_s$:

$$\begin{cases} V_{L1} = V_{PV} - V_{C1} \\ V_{L2} = V_{PV} - V_{C1} - V_{battery} \end{cases} \quad (2)$$

By using and and also voltage-second balance, the can be obtained as:

$$\begin{cases} (D)(V_{PV}) + (1 - D)(V_{PV} - V_{C1}) = 0 \\ (D)(V_{PV} + V_{C1} - V_{battery}) + (1 - D)(V_{PV} - V_{C1} - V_{battery}) = 0 \end{cases} \quad (3)$$

So the voltage gain of the converter in this mode can be calculated as:

$$M_{M1} = \frac{D}{1 - D} \quad (4)$$

Mode2:

In this mode, the power flow is from battery to motor drive system. Fig.3 shows the switches status and current of L1 and L2. From KVL identities, the voltages across inductive components L1 and L2 are obtained as:

for $0 < t < DT_s$:

$$\begin{cases} V_{L1} = V_{C1} \\ V_{L2} = V_{battery} \end{cases} \quad (5)$$

And for $DT_s < t < T_s$:

$$\begin{cases} V_{L1} = -V_{out} \\ V_{L2} = V_{battery} - V_{C1} \end{cases} \quad (6)$$

So the voltage-second balance can be written as:

$$\begin{cases} (D)(V_{C1}) + (1 - D)(-V_{out}) = 0 \\ (D)(V_{battery}) + (1 - D)(V_{battery} - V_{C1}) = 0 \end{cases} \quad (7)$$

And voltage gain of mode2 (MM2) is obtained as:

$$M_{M2} = \frac{D}{(1 - D)^2} \quad (8)$$

Mode3:

In this mode, the FC stack delivers power to load so L3 operation should be analyzed in addition to the L1 and L2. Current of inductive components are shown in Fig.4.

for $0 < t < DT_s$:

$$\begin{cases} V_{L1} = V_{C1} \\ V_{L2} = V_{battery} \\ V_{L3} = V_{FC} + V_{C3} - V_{out} \end{cases} \quad (9)$$

And for DTs < t < Ts:

$$\begin{cases} V_{L1} = -V_{C3} \\ V_{L2} = V_{battery} - V_{C1} \\ V_{L3} = V_{FC} \end{cases} \quad (10)$$

So the voltage-second balance can be written as:

$$\begin{cases} (D)(V_{C1}) + (1 - D)(-V_{C3}) = 0 \\ (D)(V_{battery}) + (1 - D)(V_{battery} - V_{C1}) = 0 \\ (D)(V_{FC} + V_{C3} - V_{out}) + (1 - D)(V_{FC}) = 0 \end{cases} \quad (11)$$

And voltage gain can be calculated as:

$$V_{out} = \frac{V_{FC}}{D} + \frac{DV_{batt}}{(1 - D)^2} \quad (12)$$

- *Mode4*

The approach of obtaining voltage gain of mode4 is similar to model1 so:

$$\begin{cases} (D)(V_{out}) + (1 - D)(V_{out} - V_{C1}) = 0 \\ (D)(V_{out} + V_{C1} - V_{battery}) + (1 - D)(V_{out} - V_{C1} - V_{battery}) = 0 \end{cases} \quad (13)$$

M_{M4} is obtained as:

$$M_{M4} = \frac{D}{1 - D} \quad (14)$$

As studied in (5), (8), (12), and (14), the converter works as a buck-boost converter in all modes, which is outstanding feature compared to other converters.

4. SIMULATION

The proposed converter is simulated in order to validate system analysis. The details of simulated system are tabulated in Table.1. In order to confirm converter features, it is simulated under different conditions in each mode.

Table 1. Simulation Specifications

Parameter	Value	Parameter	Value
V _{PV}	50(V) 40(V)	L ₃	800mH
V _{FC}	100(V) 50(V)	C ₁	1100μF
Battery Cell	80(V);25Ah	C ₂	470 μF
Motor port voltage	600(V)	C ₃	1100μF
L ₁	1200mH	C ₄	470 μF
L ₂	800mH		

The proposed converter is simulated in mode1 with two different voltages (50 and 40 V) in order to analyze its ability to regulate the battery voltage. As shown in Fig.6, it is assumed that the PV voltage decreases to 40 V at $t=1$ s. The steady state and transient of the battery port voltage are shown in Fig.6.

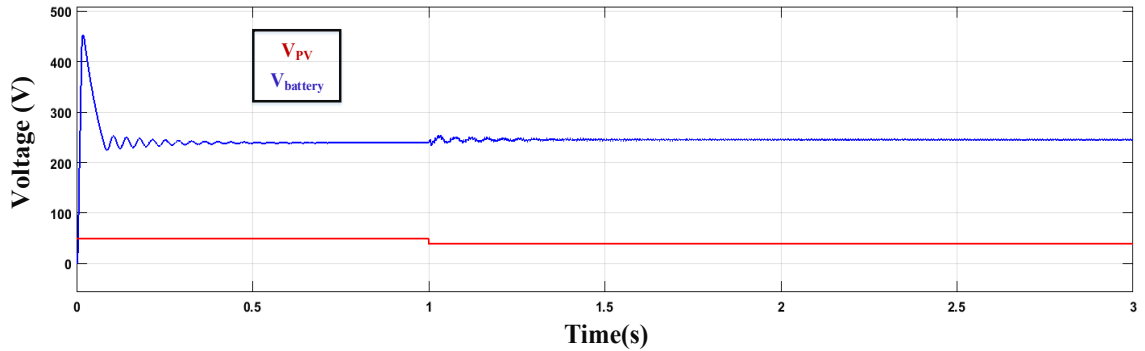


Fig. 6. PV panel and battery port voltages in mode1

The simulation is done in mode2 with two battery voltages (80 and 240V) and motor port voltage is shown in Fig.7 and Fig.8, respectively. Fig.9 illustrates the transient during switching between two battery voltages.

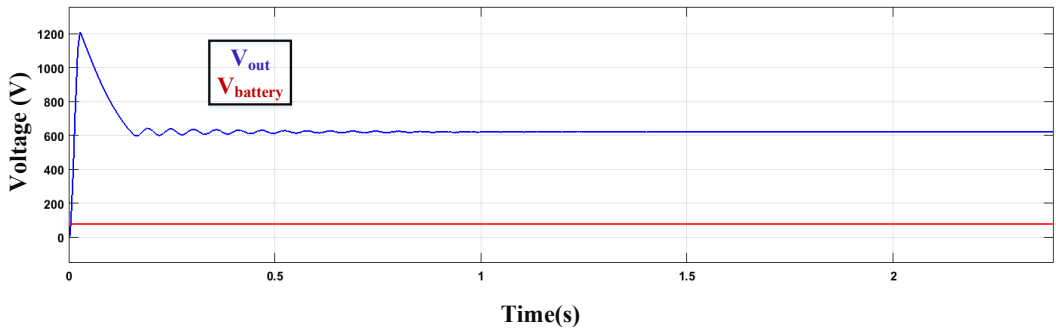


Fig. 7. Motor port voltage in mode2 with $V_{batt}=80$

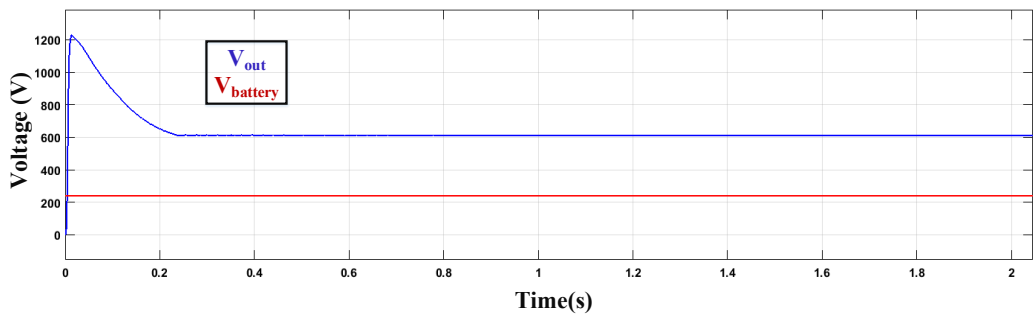


Fig. 8. Motor port voltage in mode2 with $V_{batt}=240$

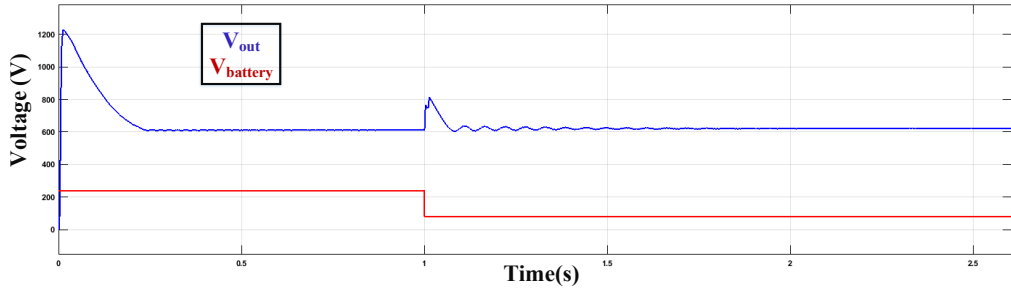


Fig. 9. Transient of Motor port voltage in mode2

The voltage and current of L1 and L2 are shown in Fig.10 and Fig.11, respectively.

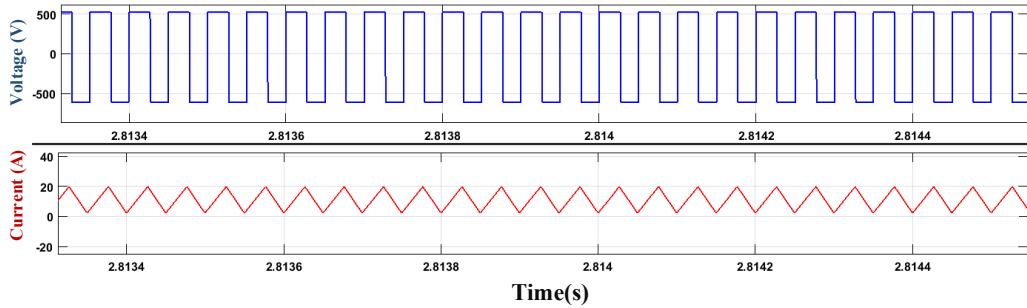


Fig. 10. Voltage and current of L1 in mode2

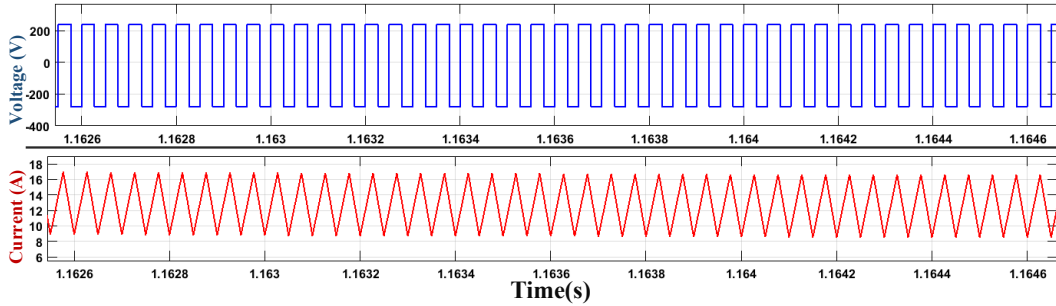


Fig. 11. Voltage and current of L2 in mode2

The V_{out} is plotted in Fig.12 with different battery and FC voltages in mode3.

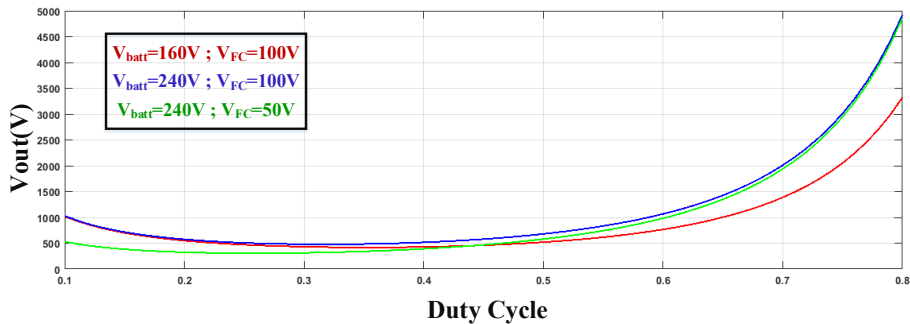


Fig. 12. Output voltage in different conditions in mode3

In order to confirm converter capability of regulating voltage, the mode3 is simulated with three battery voltages: 80V, 160V, and 240V and results are shown in Fig.13, Fig.14, and Fig.15, respectively.

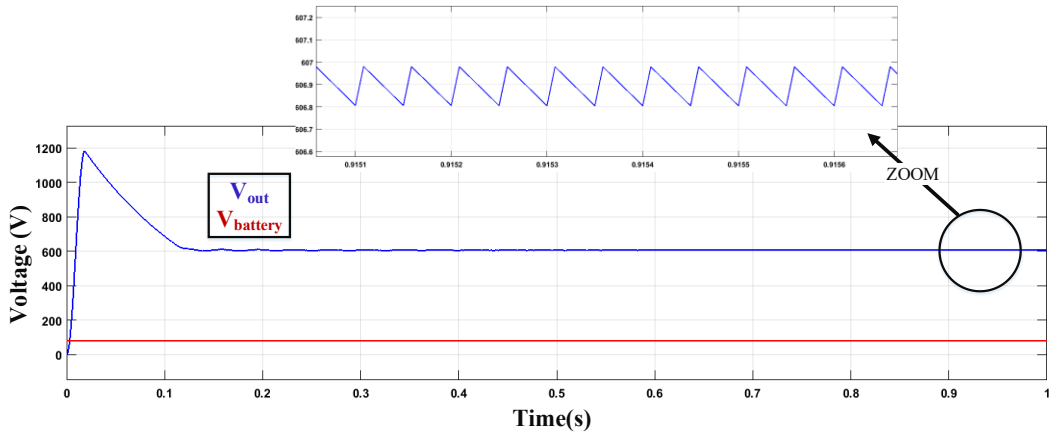


Fig. 13. Output voltage with $V_{batt}=80$ in mode3

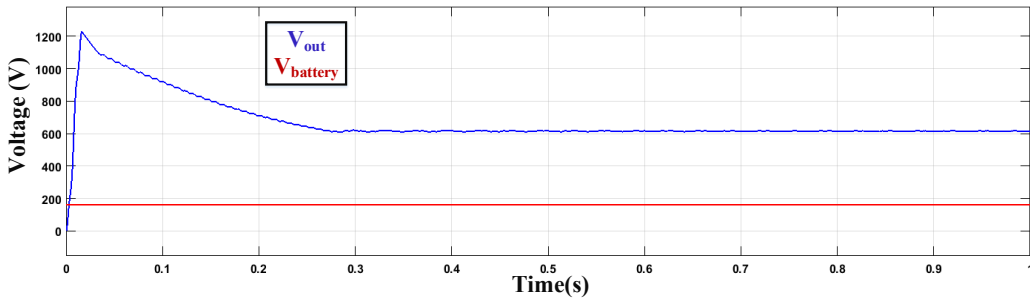


Fig. 14. Output voltage with $V_{batt}=160$ in mode3

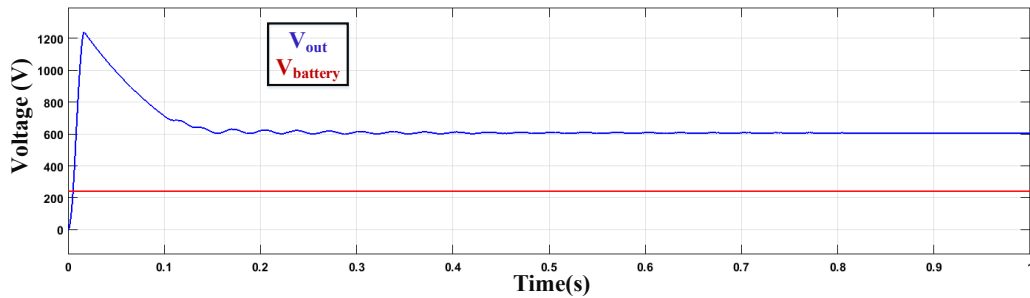


Fig. 15. Output voltage with $V_{batt}=240$ in mode3

Fig.16 shows the dynamic response of converter during switching between two battery voltages in mode3 (240 and 80V).

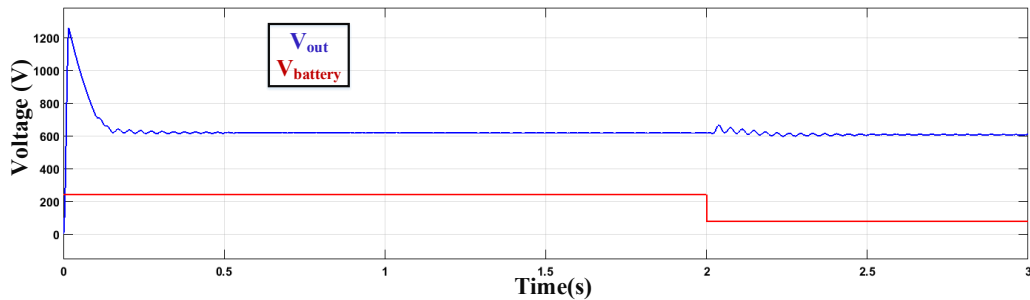


Fig. 16. Output voltage with during condition switching in mode3

The voltage and current of L1, L2, and L3 are shown in Fig.17, Fig.18, and Fig.19, respectively.

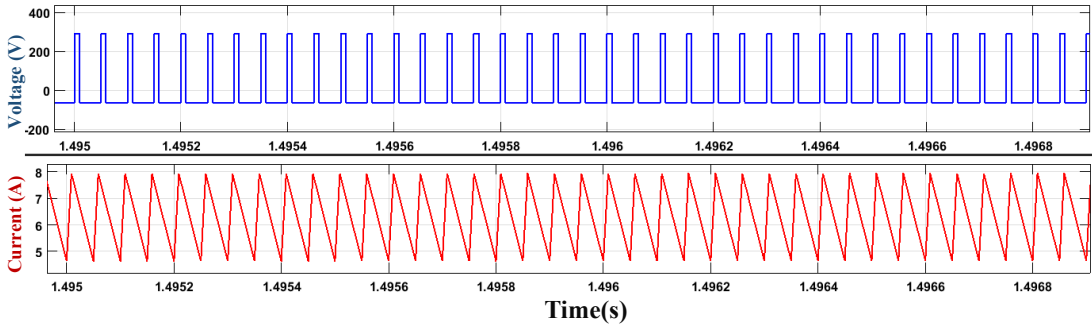


Fig. 17. Voltage and current of L1 in mode3

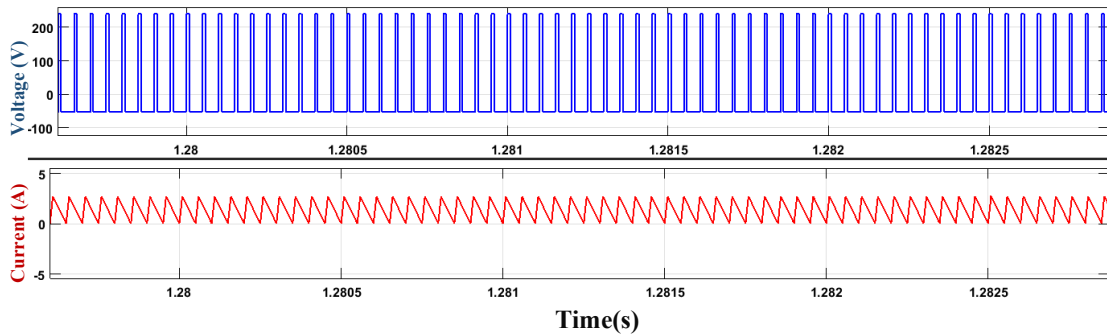


Fig. 18. Voltage and current of L2 in mode3

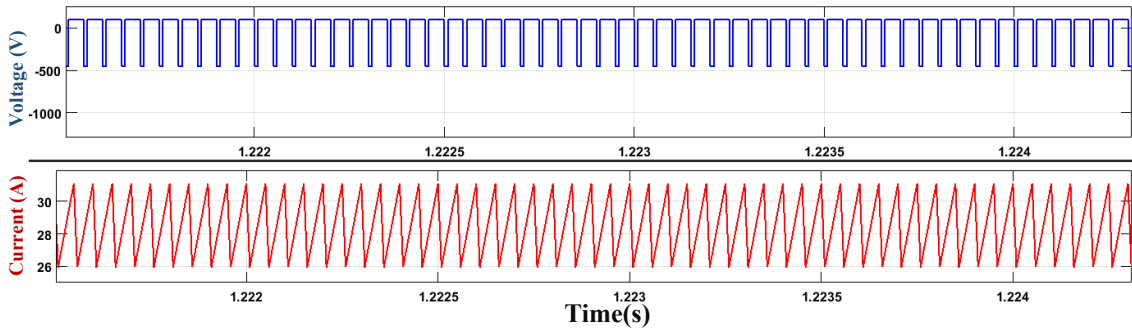


Fig. 19. Voltage and current of L3 in mode3

Switching between propulsion and braking is a very critical point in PCHEVs. Fig.20 shows the ability of converter to switch between propulsion and braking condition.

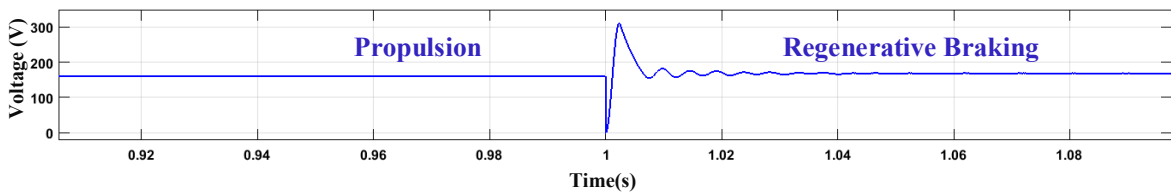


Fig. 12. Battery port voltage during switching between propulsion and regenerative braking conditions

5. CONCLUSION

The paper introduces a novel three-port bidirectional buck-boost converter designed for application in hybrid powertrains. This converter exhibits versatility by operating seamlessly in charging, propulsion, and regenerative

braking modes across a broad range of voltage levels. The inherent buck-boost structure of the converter allows for the efficient recovery of regenerative braking energy under various braking conditions. The converter's adaptability is further highlighted by its ability to supply the motor drive system with power from one or two sources, in accordance with commands from the Energy Management System (EMS).

The paper provides a comprehensive explanation and detailed analysis of all operating modes, shedding light on the converter's functionality across different scenarios. To validate its capabilities, the presented converter undergoes simulation using MATLAB software in various modes and conditions. The results from the simulation affirm the converter's features and confirm its effectiveness in addressing the diverse requirements of hybrid powertrains. This research contributes to advancing the field of powertrain technology by introducing a versatile and efficient converter with applications in charging, propulsion, and regenerative braking.

Transparency Statement

The data supporting this study are available upon reasonable request to the corresponding author, subject to ethical and confidentiality considerations.

Acknowledgments

We would like to express our gratitude to all individuals who contributed to this project.

Declaration of Interest

The authors declare that they have no competing interests.

Funding

This research received no specific grant from any funding agency, commercial, or not-for-profit sectors.

REFERENCES

- [1] Chan, C.C., Chau, K.T.: 'An overview of power electronics in electric vehicles', *IEEE Trans. Ind. Electron.*, 1997, 44, (1), pp. 3–13
- [2] Xiao, Y., C. Liu, and F. Yu, An Integrated On-Board EV Charger with Safe Charging Operation for Three-Phase IPM Motor. *IEEE Transactions on Industrial Electronics*, 2018. 66(10): p. 7551-7560.
- [3] Verma, A. and B. Singh, Multi-objective reconfigurable three phase off-board charger for EV. *IEEE Transactions on Industry Applications*, 2019.
- [4] C. C. Chan, "The state of the art of electric, hybrid, and fuel cell vehicles," *Proc. IEEE*, vol. 95, no. 4, pp. 704–718, Apr. 2007.
- [5] International Energy Agency Implementing Agreement on Hybrid and Electric Vehicles, "Outlook for hybrid and electric vehicles," IA-HEV Outlook, Jun. 2008. [Online]. Available: http://www.ieahev.org/pdfs/iahev_outlook_2008.pdf
- [6] M. Eshani, Y. Gao, S. E. Gay, and A. Emadi, *Modern Electric, Hybrid Electric, and Fuel Cell Vehicles*. New York: CRC, 2005.
- [7] H. Chen, H. Kim, R. Erickson, and D. Maksimovic, "Electrified automotive powertrain architecture using composite dc-dc converters," *IEEE Transactions on Power Electronics*, vol. PP, no. 99, pp. 1–1, 2016.
- [8] Zhang, Yong, et al. "A Soft-Switching Bidirectional DC–DC Converter for the Battery Super-Capacitor Hybrid Energy Storage System." *IEEE Transactions on Industrial Electronics* 65.10 (2018): 7856-7865.

- [9] Zhang, Yun, et al. "A switched-capacitor bidirectional DC–DC converter with wide voltage gain range for electric vehicles with hybrid energy sources." *IEEE Transactions on Power Electronics* 33.11 (2018): 9459-9469
- [10] Kumar, Bussa Vinod, R. K. Singh, and R. Mahanty. "A modified non-isolated bidirectional DC-DC converter for EV/HEV's traction drive systems." 2016 IEEE International Conference on Power Electronics, Drives and Energy Systems (PEDES). IEEE, 2016.
- [11] Zhang, Yun, et al. "Hybrid switched-capacitor/switched-Quasi-Z-source bidirectional DC–DC converter with a wide voltage gain range for hybrid energy sources EVs." *IEEE Transactions on Industrial Electronics* 66.4 (2018): 2680-2690.
- [12] Patil, D., Sinha, M., Agarwal, V.: 'A CuK converter based bridgeless topology for high power factor fast battery charger for electric vehicle application'. *IEEE Transportation Electrification Conf. Expo (ITEC)*, 2012, pp. 1–6
- [13] Patil, D., Agarwal, V.: 'Compact onboard single-phase EV battery charger with novel low-frequency ripple compensator and optimum filter design', *IEEE Trans. Veh. Technol.*, 2016, 65, (4), pp. 1948–1956